$Ni_{60}Nb_{40}$ Nanoglass: An Unconventional Non-enzymatic Glucose Sensor

Soumabha Bag*[1†], Ananya Baksi[1†], Sree Harsha Nandam[1], Di Wang[1,2], Xing-Long Ye[1], and Horst Hahn*[1,2]

Address: [1]Institute of Nanotechnology, Karlsruhe Institute of Technology, 76344 Eggenstein-Leopoldshafen, Germany

[2]Karlsruhe Nano Micro Facility, Karlsruhe Institute of Technology, 76344 Eggenstein-Leopoldshafen, Germany

[†]These authors contributed equally

Email: Soumabha Bag - soumabha.bag@kit.edu and

Horst Hahn - horst.hahn@kit.edu

* Corresponding author

Abstract

Although nickel based nanomaterials are mostly used for non-enzymatic glucose sensing due to unique property of nickel to oxidize glucose reversibly, long term stability and organic ligand protection on the nanoparticle surface restrict their usage for the commercial purpose. Here we report an unconventional nickel-niobium ($Ni_{60}Nb_{40}$) amorphous alloy for glucose sensing in alkaline medium for the first time. Three different systems comprising of $Ni_{60}Nb_{40}$ atomic composition, having completely different microstructures were used for the current study and their glucose sensing ability is tested at various electrochemical conditions. Among melt-spun-ribbon, *nanoglass* and amorphous-crystalline nanocomposite materials, *nanoglass* showed the best performance in terms of high anodic current density, sensitivity (20 mA . cm^{-2} . mM^{-1}), limit of detection (100 nM glucose), stability and reproducibility (above five thousand cycles), and sensing accuracy to be developed as a non-enzymatic glucose sensor using amorphous alloys. Phase, chemical composition and microstructures of these reacted alloys remain unchanged even after several cycles. When annealed in vacuum, only the heat-treated *nanoglass* retained the similar electrochemical-sensing property while the other materials fail for the purpose. Plausibly, microstructural modification of the materials upon introducing network of interfaces through the consolidation of glassy grains in the pellets, compared to melt-spun-ribbon, is responsible for the remarkable improvement of chemical reactivity of the nickel towards glucose.

Keywords

Nanoglass, non-enzymatic glucose sensor, nickel-niobium alloy, cyclic voltammetry, electrochemistry

Introduction

Accurate glucose detection ability is essential to capture small change in concentration in order to design advanced clinical diagnostic device[1, 2] (blood sugar analysis apparatus[2-5] and other personal health care device[6]). Besides clinical applications, environmental[7], food[8] and drug quality inspection[1, 9, 10], bio-processes[11, 12] monitoring are carried out upon evaluating glucose reactivity. In order to accommodate all the above-mentioned requirements, constant efforts are made to develop a universal sensor, which will be fast, selective, reliable, cost-effective, user friendly and efficient. Initially, Clark and Lyons[13] designed enzyme based electrode using specific biocatalytic property of glucose oxidase or GOx, which was further improved for the development of redox electrode[14] towards clinical diagnosis aimed for diabetes control. Despite its success, enzymatic glucose sensors possess several problems to address such as, immobilization of GOx on electrode[15, 16], long-time stability[17], thermal and chemical stability[18], handling and repeated use of the same sensor. Besides clinical diagnostics, limited range of thermal stability[18, 19] (till 44 °C) of GOx-based sensors along with its unstable nature in lower (below 2) and higher (above 8) pH values[15], makes it a poor choice to develop sensor for commercial use in agriculture and food quality monitoring[10]. In order to address the above-mentioned problems, immense efforts are made to develop effective non-enzymatic glucose sensing technology based on metals and nanomaterials.

Among different diagnostic patterns invented to monitor glucose concentrations, such as, transdermal technology[20], optical[12, 21] and acoustic[22], electrochemistry[4, 23] based diagnostic tools has been found to be the most efficient and user friendly. Application based on chemical reactivity of glucose is the origin to develop electrochemical non-enzymatic glucose sensor. Generally, electrodes made of noble metals, such as gold[24], silver[25], palladium[26], and platinum[27] are used to produce enzyme free glucose sensors in spite of the high cost. But, all these emerging sensors have been unable to demonstrate comparable sensitivity of GOx-based detectors mainly due to poor electro-oxidation kinetics; despite introducing anisotropic nanostructured electrodes[28] or alloying[17, 29] during the design of the electrode. Therefore, readily available, cost effective transition metal[5, 17] catalysts are selected to design the futuristic enzymeless glucose sensor. Among known metal catalysts, nickel based materials (nickel nanoparticle decorated substrate[30], anisotropic Ni-structures[17], multi component alloys[15, 31, 32, 33] or hybrid structures[34] containing nickel) are chosen because of stable and reversible Ni(III)/Ni(II) redox system[17, 35] activity known in alkaline condition. However, during electro-chemical oxidation of glucose, such Ni-based sensors' performance and stability decline over time. Above-mentioned challenges can be addressed by designing a new type of ligand free Ni based sensor which is stable to survive several electrochemical cycles, easy to handle but able to detect very low concentration of glucose reproducibly.

Nanostructured metallic glasses are known for their unique properties[36, 37, 38-40] compared to bulk metallic glassy[41] analogue. Recent introduction of *nanoglass*[40] in the family of glassy alloys further improved the mechanical strength[39, 42], enhanced magnetic properties[37, 43] etc. compared to bulk metallic glasses. Typically, *nanoglass* is made by consolidating alloy nanoparticles at high uniaxial pressure (2-6 GPa)[44] creating large number of interfaces which is responsible for their distinct properties[45] compared to bulk metallic glass of similar

composition. While stable metallic glasses are being used in several places[46], only a few attempts are made (organic catalyst[47], electrocatalysis[48], and sensor[33, 38]) to utilize chemical reactivity of such amorphous systems as replacement to crystalline metals. Nickel based glasses like $Ni_{60}Nb_{40}$[49], $Ni_{60}Zr_{40}$[50, 51], $Ni_{60}Ag_{40}$[52], $Ni_{50}Ti_{50}$[53] are well-known for their distinct thermal stability and mechanical strength but they have not been used significantly for unconventional chemical applications[54]. These nickel-based glasses could be excellent choice to develop futuristic non-enzymatic glucose sensors.

In this paper, we demonstrate a remarkable electro-oxidation performance in terms of sensitivity and selectivity of $Ni_{60}Nb_{40}$ metallic and *nanoglass* (amorphous alloy) in glucose sensing. Three types of alloys (melt-spun-ribbon, *nanoglass* and nanocomposite of amorphous and crystalline alloy) with identical compositions ($Ni_{60}Nb_{40}$) have been investigated for their electrochemical activity towards glucose sensing. Results from the investigations reveal that all of these $Ni_{60}Nb_{40}$ alloys can effectively be used to detect glucose electrochemically in absence of any enzyme. Among them, *nanoglass* showed the highest sensitivity (20 mA . cm^{-2} . mM^{-1}) reported so far for any non-enzymatic glucose sensor based on Ni-based nanomaterials.

Materials and Methods

Chemicals: $Ni_{60}Nb_{40}$ target (99.9% purity) was purchased from MaTeck GmbH. Glucose (99% purity) was procured from VWR GmbH. Sodium hydroxide (NaOH), ascorbic acid, sodium chloride (NaCl), sucrose with 99.9% purity were purchased from Sigma-Aldrich. MilliQ water (18.3 MΩ) was used throughout the experiments.

Synthesis: Synthetic schemes are illustrated in Figure 1 (A to C). Briefly, melt-spun-ribbon (MSR) was prepared by rapid quenching of molten mixture of Ni and Nb with 60:40 atomic ratio on a rotating Cu disk. Other samples were synthesized using inert gas condensation (IGC) techniques followed by compaction in two custom-built instruments. $Ni_{60}Nb_{40}$ *nanoglass* was prepared by using magnetron sputtering-IGC (MS-IGC) followed by compaction at 1.4 GPa in vacuum[39]. With this method, $Ni_{60}Nb_{40}$ alloy target was sputtered at an aggregation pressure of 0.3 mbar, which leads to the formation of very fine nanoparticles of the same composition. The nanoparticles were then collected and pressed *in-situ* at a pressure of 1.4 GPa to make a disc shaped pellet. The sample was further consolidated at 6 GPa and polished mechanically in ambient condition before studying its electro-oxidation property. The amorphous-crystalline nanocomposite sample was prepared using pulsed laser (20 W laser power) ablation (on same $Ni_{60}Nb_{40}$ alloy target) setup coupled to IGC instrument followed by successive consolidation at 1.8 GPa and 6 GPa. A disc shaped pellet was prepared and polished similar to the previous *nanoglass* sample. The use of pulsed laser ablation instead of magnetron sputtering in the IGC system induced nano-crystallinity in the compacted pellet.

Electrochemical Cell Configuration: All the electrochemical (cyclic voltammetry and chronoamperometry) experiments were performed in a general-purpose electrochemical system (from μAutolab Type III) coupled with three-electrode electrochemical cell, where $Ni_{60}Nb_{40}$ alloys were used as working electrode, platinum foil as counter electrode and saturated Ag/AgCl as reference electrode. A gold wire of 0.50 mm thickness was used to connect working electrodes.

Cyclic Voltammetry and Chronoamperometry: Cyclic voltammetric (CV) studies were performed with different concentrations of glucose solutions (100 nM to 38 mM, generated more than few thousand CV sweeps with single *nanoglass* electrode) prepared in 0.1 M NaOH at room temperature (25 °C) in a 50 mL cell. Scan voltage was fixed between -0.1 to +0.45 V to avoid any interference emerging from niobium. During chornoamperometric measurement, glucose, ascorbic acid, sodium chloride (NaCl) and sucrose solutions were added into 0.1 M NaOH solution sequentially with constant stirring at 200 rpm. Geometric surface area of the working electrodes (alloys) was used to calculate the current density values reported here. All the potential values described in this paper were determined with respect to saturated Ag/AgCl electrode (+0.194 V vs. SHE).

Characterization: Conventional characterization techniques were used to determine the phase, composition of the as-prepared materials. Structural characterization (XRD) of the metallic alloys was carried out using a Bruker X-ray diffractometer equipped with a Cu Kα X-ray source before attempting electrochemical studies. A STOE Stadi P diffractometer with Ga-Kβ source was used for Ga-XRD characterization of the reacted electrode. Microstructure analysis was performed using a Zeiss LEO 1530 scanning electron microscope (SEM) and an image aberration corrected FEI Titan 80-300 transmission electron microscope (TEM) operated at 300 kV. Elemental analysis and chemical compositions ($Ni_{60}Nb_{40}$) were determined with an energy dispersive X-ray spectroscopy (EDX) detector attached to the SEM and TEM instruments. X-ray photoelectron spectroscopy (XPS) measurement was carried out in an ECSA probe TPD spectrometer from Omicron Nanotechnology with polychromatic Al Kα (hν = 1486.6 eV) as X-ray source. All XPS spectra were deconvoluted and analysed using CasaXPS software.

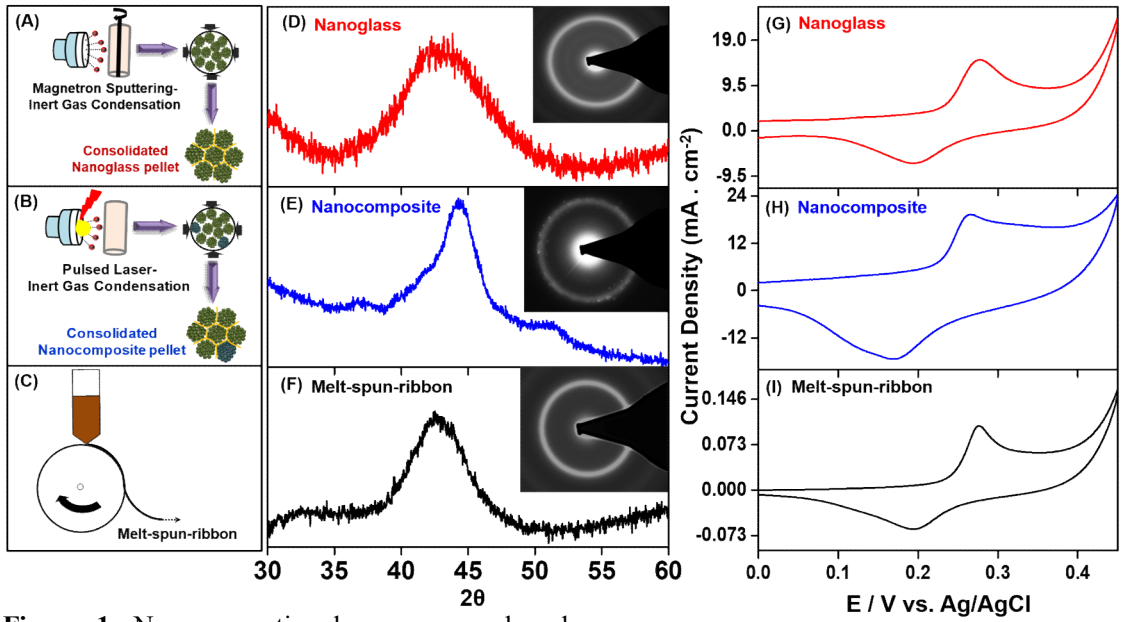

Figure 1: Non-enzymatic glucose sensor based on $Ni_{60}Nb_{40}$ glassy alloy materials is illustrated. Schematics in A to C show preparation methods of *nanoglass*, nanocomposite, and melt-spun-ribbon, respectively. XRD analysis indicate amorphous phase of the sample (D and F), which are further confirmed through SAED patterns shown inside the insets. Glucose detection ability of the materials are measured in 0.1 mM glucose prepared in 0.1 M sodium hydroxide solution in cyclic voltammetry which are shown in G – I.

Results and Discussion

Structural characterizations of the as-prepared samples are performed using X-ray diffraction (XRD) immediately after each synthesis. Corresponding diffractograms associated with each material are shown in Figure 1D to 1F. Both *nanoglass* and melt-spun-ribbon (MSR) show typical halo peak indicating mostly amorphous phase in the samples. Detailed microstructure analysis by TEM further confirmed the amorphous nature of the samples where selected area electron diffraction (SAED) exhibit broad diffuse rings as shown in Figure 1D and 1F. Although there was no clear crystalline peak in the XRD pattern (amorphous-crystalline composite or nanocomposite), the halo was sharper for the nanocomposite materials suggesting slight nano-crystallinity (inset of 1E). Additionally, some distinguished spots identified on SAED pattern indicate some extent of nano-crystallinity in the sample.
After initial microstructural characterization, these three samples were tested for their electrochemical responses as working electrode towards glucose in cyclic voltammetry (CV) experiments in alkaline medium. Scan rate dependent stability of the electrodes have been checked before initiating any experiment. Initial optimization was performed with crystalline Ni, which showed poor and irreversible response in 0.1 M NaOH solution. Subsequent attempt with the polished glassy electrode, during sweeping from -0.1 V to +0.45 V at 10 mV . s^{-1} scan rate, oxidative peak in the first cycle indicate the formation of Ni(II) oxide layers[32]. Repeated sweeps from 10 mV . s^{-1} to 100 mV . s^{-1} rates, *nanoglass* electrode produced well-defined and reproducible voltammograms in 0.1 M NaOH solution as shown in Figure S1. Other alloy electrodes also generate similar voltammetric response. Anodic peak voltage shifts to positive value with increase in scan rate while reductive peak voltage move to negative potential as found in previous studies. During sweeping at 20 mV . s^{-1} rate, current response was found to be 0.64 μA for the anodic peak at +0.266 V and the cathodic peak voltage was found at +0.179 V. The scan rate was fixed at 20 mV . s^{-1} for the rest of the experiments. The reactions are as follows:

$Ni + 2OH^- \rightarrow Ni(OH)_2 + 2e^-$
$Ni(OH)_2 + OH^- \rightarrow NiO(OH) + H_2O + e^-$
$NiO(OH) + Glucose \rightarrow Ni(OH)_2 + H_2O + Glucolactone$

In the identical potential regime for *nanoglass*, upon addition of 0.1 mM glucose solutions into the alkaline medium, substantial increase in the oxidative peak current was identified in the resultant CV curve as evident in Figure 1G and anodic peak potential shifts to higher voltage. Notable enhancement in anodic peak current is due to the electrochemical oxidation of glucose in presence of Ni(O)OH on the electrode surface. However, this glucose oxidation step is irreversible in nature as confirmed from the reverse sweep where minimal current change is observed without any shift in the reduction peak position. It should be noted here that although the *nanoglass* does not have any surface protection, it is highly stable in alkaline condition for months and provides reproducible signal for over 5000 cycles.

Comparable sensitivity was measured when the electrode was replaced with nanocomposite (shown in Figure 1H). Although MSR was able to detect 0.1 mM glucose in solution, weaker oxidative peak current response was seen which makes it unsuitable for a glucose sensor at the low concentration window (Figure 1I).
Appropriate glucose diagnosis is formulated with further CV experiments with different batches of solutions. Gradual increase in oxidative peak current values with increase in glucose concentrations (0.1 to 0.5 mM) clearly indicates the proper sensing response of the *nanoglass* (Figure 2A). Eight replicates of voltammograms from 0.1 mM glucose solution,

showed in Figure 2B, confirms reproducible nature of the measurements with stable anodic peak current as shown in the inset. Identical measurements are performed on the composite and MSR and sensitivity of these materials is checked with varying glucose concentrations. A linear relationship is found when the anodic peak current density is plotted against glucose concentration (0.1 to 2 mM) and the sensors performances are evaluated for all three alloys (Figure 2C). The sensitivity of the alloy sensors are calculated from the slopes in Figure 2C. It is evident from the plots that the response of the *nanoglass* and the nanocomposite are found to be better than MSR. Although the nanocomposite material shows comparatively higher current density for lower glucose concentration, the current density do not increase tremendously with higher glucose concentration and hence the overall sensitivity of nanocomposite materials is lower than the *nanoglass* (Figure 2C).

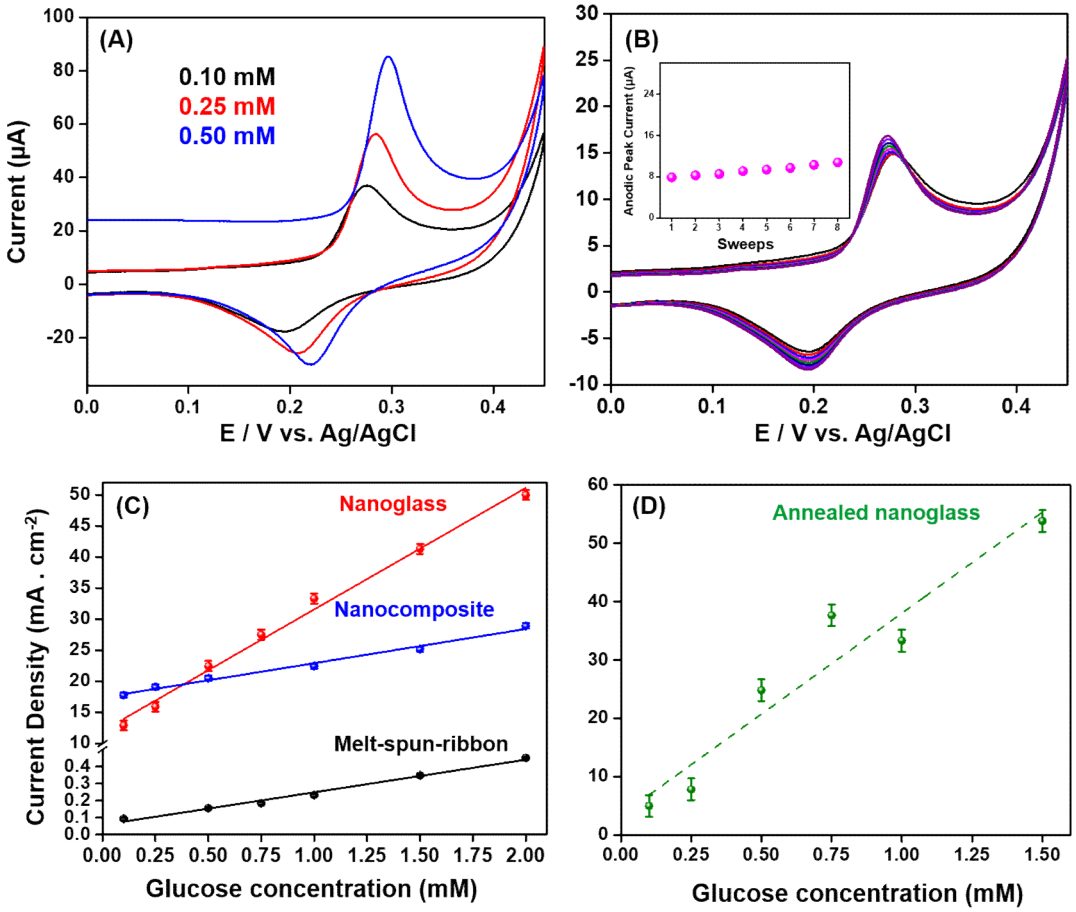

Figure 2: Stability and reproducibility of the sensors are determined. Concentration dependent (0.10, 0.25 and 0.50 mM glucose) cyclic voltammograms with *nanoglass* is shown in A. In B, eight sweeps in 0.1 mM glucose solution demonstrate stable anodic peak current (as shown in inset). Analogous study with nanocomposite and MSR also produce concentration dependent linear response with respect to anodic peak current density (represented in C). Only annealed *nanoglass* retained its detection ability and its response, which is captured in D.

The sensitivity of the *nanoglass* is found to be 20 mA . cm^{-2} . mM^{-1}, which is substantially higher among the reported nickel based glucose sensors[15]. The sensitivity of the nanocomposite materials and MSR are 5.5 and 0.2 mA . cm^{-2} . mM^{-1}, respectively. Current density as well as sensitivity is found to be the lowest for melt-spun ribbon among all the three alloys. It is interesting to note that all the three material showed nearly linear behavior in terms of current response with respect to glucose concentration.

In order to gain more insight into the phase dependent reactivity of the materials; all sensors are first annealed at 700 °C [above its glass transition temperature (T_g), 622 °C] for two hours in a vacuum furnace. Upon crystallization, several phases appear from a single-phase $Ni_{60}Nb_{40}$ amorphous alloy[55]. Besides metallic nickel, a mixture of intermetallic compounds of nickel and niobium (Ni_3Nb, Ni_6Nb_7)[51] are produced from *nanoglass* (Figure S2). When the CV of all the annealed (crystallized) electrodes are tested, only annealed *nanoglass* showed reproducible current density comparable to the parent *nanoglass*. However, the high sensitivity is lost (Figure 2D) in the heat-treated *nanoglass* while other materials do not respond at all and fail to produce any anodic peak current. Although the current density is higher for annealed *nanoglass* (with respect to parent *nanoglass*), the linear behavior is no more perfect (adj. R^2 = 0.905 compared to adj. R^2 = 0.992 for pristine *nanoglass*, 0.986 for nanocomposite and 0.986 for MSR, respectively). This study clearly proves the weak sensitivity of the crystalline materials in non-enzymatic glucose sensing in alkaline medium. Due to remarkable response (pristine and annealed sample), further studies are focused on *nanoglass* only.

To find out the limit of detection with *nanoglass*, chronoamperometric experiments are performed from lowest to highest concentration of glucose and the results are shown in Figure 3. During the measurement, the potential is held constant at +0.45 V while the solution is stirred constantly (200 rpm rate) and current is monitored upon successive addition of glucose

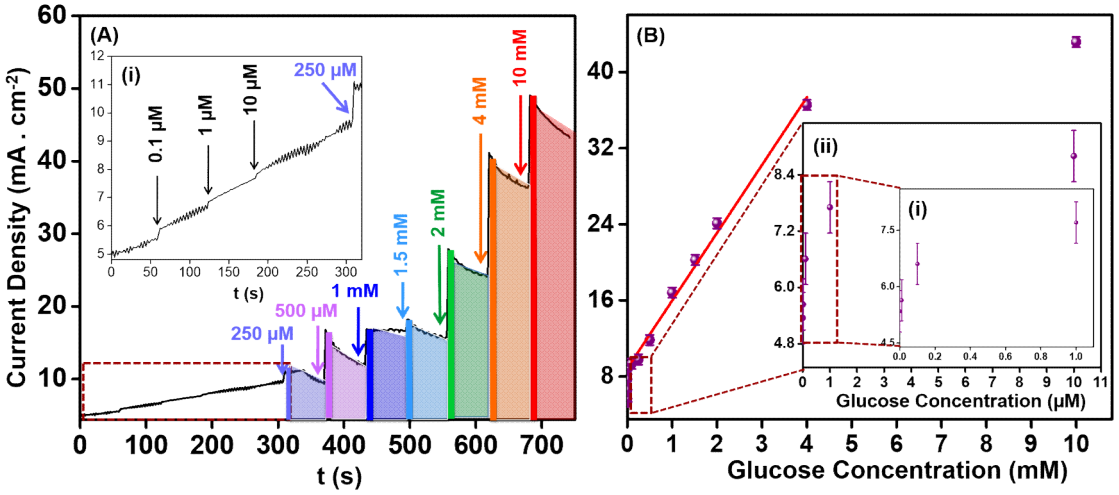

Figure 3: (A) Chronoamperometric response from *nanoglass* electrode upon sequential addition of glucose solutions. Inset (i) shows the expanded view of red dotted region. Distribution of current densities with respect to glucose concentration is shown separately in (B). A linear increase of current density is established from 0.25 mM to 4 mM. Current densities at lower concentration are given in insets (i) and (ii).

solutions into 0.1 M NaOH medium. Well-defined stepwise current increase upon sequential addition of glucose proves accurate electro-oxidation response of *nanoglass* as working electrode. Above 10 mM glucose concentration, negligible increase of current is identified; therefore, concentration range of present investigation is chosen till 10 mM. Plausibly, all the active sites available on the *nanoglass* get occupied by the reaction intermediates at this concentration, leaving little room for additional glucose molecule adsorption for the electro-oxidation process to take place. Another reason could be use of Ag/AgCl electrode as counter electrode. At higher glucose concentration in alkaline medium, it can reduce Ag(I) to Ag(0) and the metallic Ag redeposit on the electrode surface making it non-acceptable as a reference electrode. Based on signal to noise ratio (S/N) calculation, *nanoglass* offers 100 nM glucose solution as limit of detection (LOD) as shown in the inset of Figure 3A. A linear increase of

current density with respect to glucose concentration has been established between 0.25 mM to 4 mM when chronoamperometric current densities are plotted against glucose concentration (Figure 3B). Due to high current density, a few nanomolar glucose is also detectable as shown in Figure 3Bi and 3Bii, which also supports proper detection ability of *nanoglass* at lower concentration range.

In order to demonstrate the ability of *nanoglass* as enzyme free glucose sensor for future, selectivity is another important factor alongside sensitivity, which has to be taken into consideration. Mostly glucose detection is hampered by the presence of sucrose, ascorbic acid and other solutes in the blood stream. To perform this, 0.25 mM ascorbic acid, sodium chloride (NaCl), sucrose solutions are added in succession (Figure S3A) in 0.25 mM glucose solution. Marginal current change upon the addition of other solutes confirms the good selectivity of the *nanoglass* for glucose. This control test reveals *nanoglass* has potential for accurate glucose detection and it can be used as non-enzymatic glucose sensor in future. In addition to its selectivity towards glucose detection, chronoamperometric response of *nanoglass* for

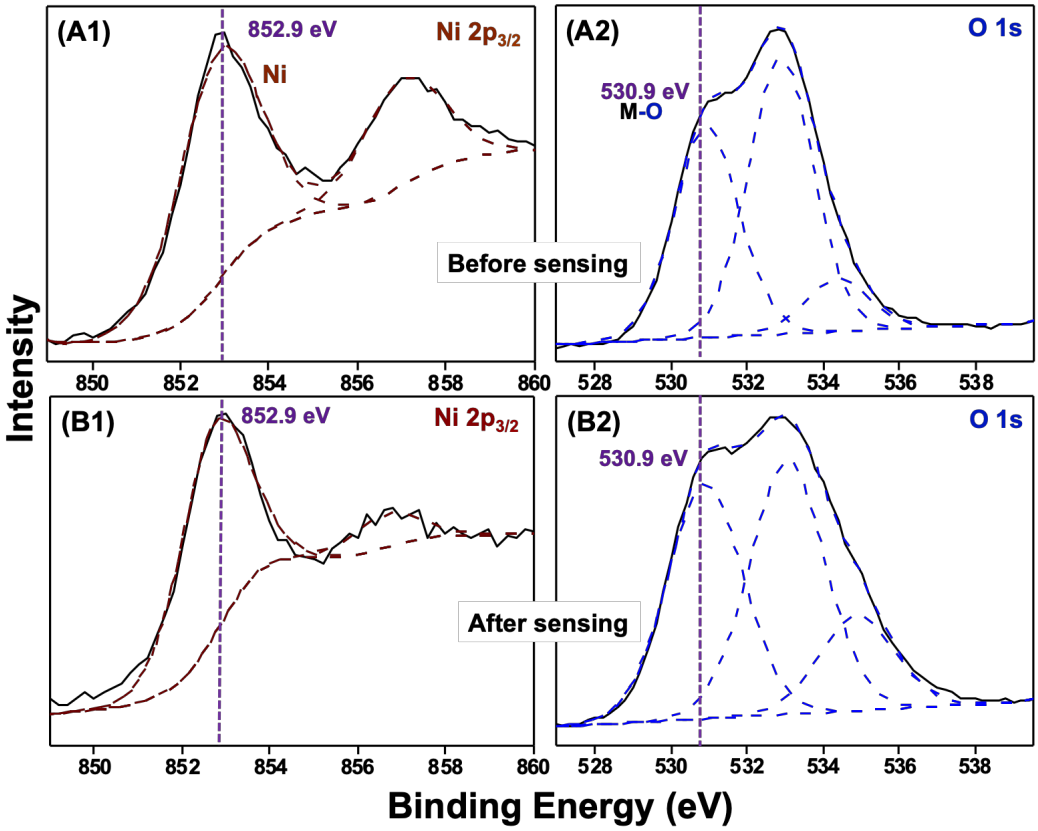

Figure 4: XPS measurement of the *nanoglass* electrode before (A1 and A2) and after (B1 and B2) detection experiments, highlighting Ni 2p and O 1s regions. Similar features in the fitted and deconvulated spectra (dashed lines) confirm unchanged surface composition.

the sensing of higher glucose concentrations (2 mM to 38 mM) has also been tested independently (Figure S3B). In identical chronoamperometric experiment (applied potential +0.50 V), current increases linearly (adj. R^2 = 0.996) with infusion of higher concentration of glucose till 38 mM. However, above 10 mM, continuous cleaning of the reference electrode has been carried out before additional infusion of glucose solution. This problem can be avoided by using suitable reference electrode, replacing Ag/AgCl.

Following the electro-oxidation studies, structural analysis of *nanoglass* electrode is carried out with Ga-XRD to understand the active phase present on its surface. Resultant diffractograms before (Figure S4A) and after (Figure S4B) reaction showed identical featureless broad peak, indicating retention of amorphous phase in the alloy even after electro-oxidation experiments. XRD patterns shown in Figure 1D and Figure S4A are collected from the same sample. Subsequently, surface characterization of the *nanoglass* is carried out by XPS to determine chemical composition. While Figure 4A1 and 4A2 represent Ni ($2p_{3/2}$) and O (1s) regions of unreacted *nanoglass* samples, same regions of the reacted samples are shown in Figure 4B1 and B2. Upon deconvoluting Ni $2p_{3/2}$ regions (in Figure 4A1 and 4B1) nearly same features are found which indicates unaltered nickel composition at the surface of the electrode. Careful analysis of O 1s region points towards different metal-oxygen bonding possibilities at the *nanoglass* surface (Figure 4A2 and B2), which also do not change significantly following electro-oxidation process. These features appear mainly due to presence of amorphous niobium oxide at the surface of the sample, recognized by XPS analysis in Nb 3d region (Figure S5). Two oxidation states of Nb are found upon deconvoluting two indistinguishable (Figure S5A and B) spectra measured before and after sensing experiments, respectively. Peak at 203.86 eV is attributed to NbO while Nb_2O_5 $3d_{5/2}$ signal appears at 207.62 eV. It should be noted that presence of niobium oxide at the surfaces of *nanoglass* had not been identified either by XRD or during TEM/SAED analysis (Figure 1D). Appearance of Ni, Nb and O peaks from metallic *nanoglass* suggests presence of niobium oxide layer at the surface, which also maintains metallic bonding with Ni[56] but protects underlying Ni-Nb layers from further oxidation. As a result of metallic bonding between Ni and NbO_x at the surface, the oxide layer and the sample remain always conducting. This niobium oxide not only facilitates the electro-chemical sensing but also shields underlying Ni-excess regions of the sample.

Mechanism

In view of all the results produced by electrochemical oxidation process and subsequent spectroscopic characterization of the materials, *nanoglass* has emerged as stable, sensitive, reliable and robust glucose detector, however, all $Ni_{60}Nb_{40}$ alloy material have the potential for glucose sensing. Principle reason for such activity is the presence of amorphous nickel with non-interfering and non-competing niobium in the material. Together these elements produce a stable yet reactive alloy electrode surface with increased reactivity towards glucose[5]. Incipient Hydrous Oxide Adatom Mediator (IHOAM)[4, 23] model can be used to explain the plausible mechanism (Figure 5) of the oxidation process. According to the previous observation, a thin layer of nickel hydroxide [$Ni(OH)_2$] forms on the electrode surface in the first sweep of electro-oxidation[32]. $Ni(OH)_2$ subsequently oxidized to nickel oxohydroxide [NiO(OH)] in alkaline medium which adsorbs glucose molecule and gradually converts to glucolactone in alkaline condition. In the process, NiO(OH) reduces to $Ni(OH)_2$ which participate in the process again (see the Figure 5 for details). Considering the experimental evidences, every working electrode in the investigations has been following common mechanism formulated using IHOAM model as shown in Figure 5. In case of annealed glasses, multi-phasic intermetallic compounds do not participate in glucose sensing. Their presence also reduces the metallic bonding between Ni-NbO_x significantly and

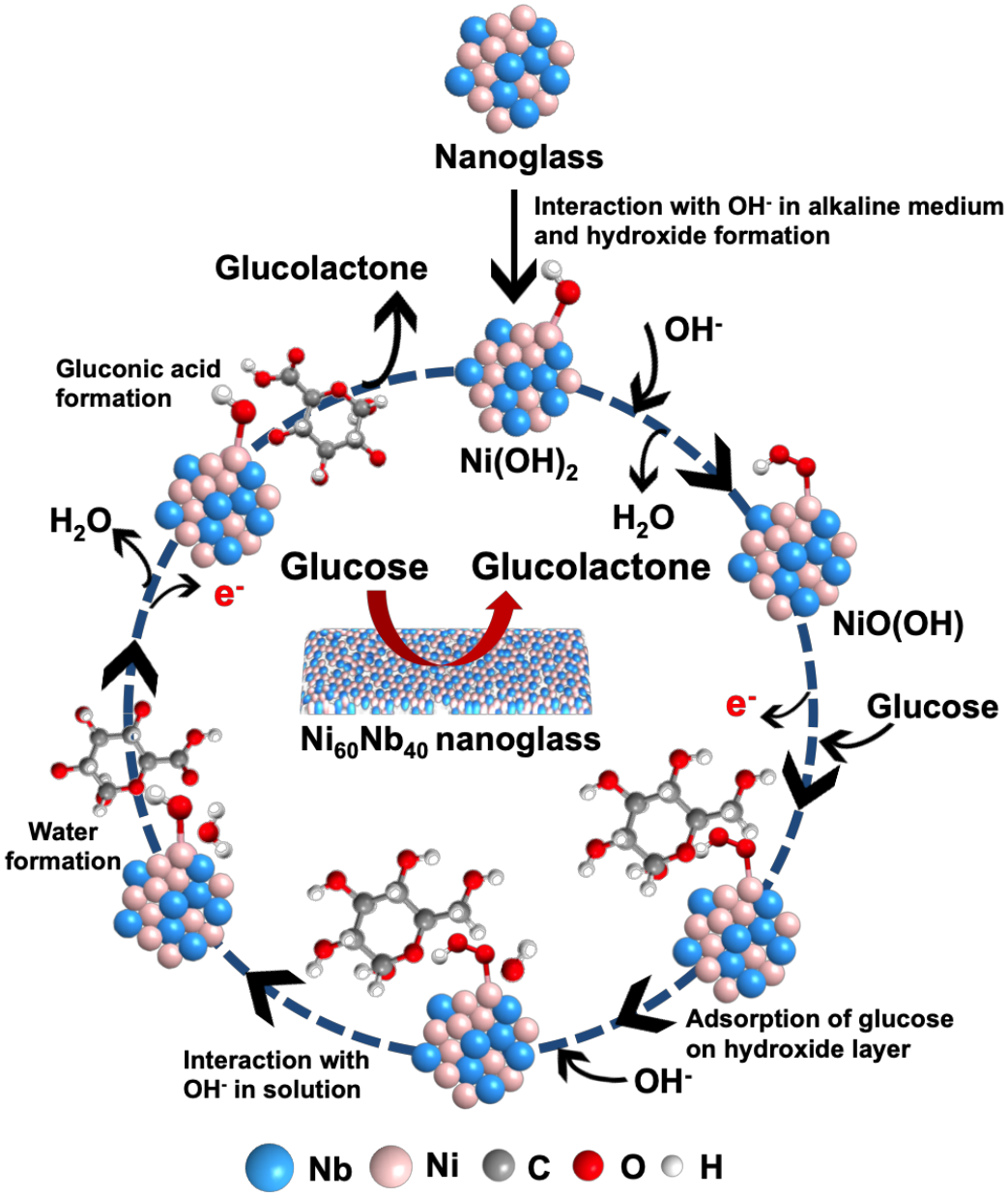

Figure 5: Proposed mechanism of electrochemical glucose oxidation process at the surfaces of $Ni_{60}Nb_{40}$ *nanoglass*.

transforms into a less conducting electrode, which is inefficient for the electrochemical sensing process.

Difference in microstructure in *nanoglass* and nanocomposite alloy compared to MSR can be another reason for the better electrochemical response among three materials. In *nanoglass* and nanocomposite samples, a network of interfaces creates nanosize islands of glassy regions, which are stapled through compaction. Interface of these glassy regions may also accommodate and enhance the electro-oxidation process. As a result, *nanoglass* and

nanocomposite materials show improved response in CV experiments compared to bulk MSR.

Conclusions

In this report, electrochemical detection of glucose has been demonstrated using nickel based glassy alloys for the first time. Fast, reproducible responses from different $Ni_{60}Nb_{40}$ metallic alloys (*nanoglass*, nanocomposite and melt-spun-ribbon) are compared for the sensing of glucose solutions. Exceptional response from *nanoglass* sample is determined which retain its partial reactivity even after annealing. Due to high current density, a few nanomolar glucose is also detectable. Besides metallic nickel's contribution, the microstructure *nanoglass* with interfacial regions of enhanced free volume (interfaces) also seems to play a role for the remarkable electrochemical reactivity. With minimum 100 nM limit of detection ability, *nanoglass* has been shown to be an unconventional, nanostructured and ligand free material for the futuristic non-enzymatic glucose sensor. Conducting niobium oxide layer coating creates a protection for Ni-rich alloy but maintains chemical reactivity towards glucose. Impressive performance of this type of unconventional yet responsive alloy-based sensor has the potential for the development of novel diagnostic apparatus and technology to monitor glucose concentrations in challenging sectors. Thorough understanding of the mechanism and further structural insights are necessary to use these materials for commercial purpose.

Acknowledgements

S.B. and A.B. gratefully acknowledge Karlsruhe Institute of Technology for guest scientist fellowships. H.H. and S.H.N acknowledge for the financial support provided by the Deutsche Forschungsgemeinschaft under grant HA 1344/30-2. Authors would like to thank Dr. Zbigniew Śniadecki from Institute of Molecular Physics, Polish Academy of Sciences for the melt-spun-ribbon sample. Dr. Ben Breitung is gratefully acknowledged for the Ga-XRD measurement.

Author contributions

A.B. and S.B. have jointly planned and performed the experiments and interpreted the results. S.H.N. had helped in magnetron sputtering experiments. D.W. performed the TEM characterization and helped in microstructure analysis. X.L.Y. helped to design initial electrochemical experiments. H.H supervised the entire project. A.B.; S.B. and H.H. wrote the manuscript.

Additional Information

The authors declare no competing financial interests. Supplementary information this paper is available on www.nature.com/naturematerials. Correspondence and requests for materials should be addressed to S.B. and H.H.

References

[1] G. Gnana kumar, G. Amala, S. M. Gowtham, RSC Adv. 2017, 7, 36949.
[2] A. Harper, M. R. Anderson, Sensors 2010, 10, 8248.
[3] A. Heller, B. Feldman, Chem. Rev. (Washington, DC, U. S.) 2008, 108, 2482.
[4] M. M. Rahman, A. J. S. Ahammad, J.-H. Jin, S. J. Ahn, J.-J. Lee, Sensors 2010, 10, 4855.
[5] K. Tian, M. Prestgard, A. Tiwari, Mater. Sci. Eng., C 2014, 41, 100.

[6] G. Alfian, M. Syafrudin, M. F. Ijaz, M. A. Syaekhoni, N. L. Fitriyani, J. Rhee, Sensors (Basel) 2018, 18.
[7] E. Bandiello, M. Sessolo, H. J. Bolink, J. Mater. Chem. C 2014, 2, 10277; K. G. Nikolaev, A. Offenhausser, Y. G. Mourzina, K. G. Nikolaev, A. Offenhausser, Y. G. Mourzina, K. G. Nikolaev, Y. E. Ermolenko, S. S. Ermakov, Front Chem 2018, 6, 256; N. P. Sardesai, A. Karimi, S. Andreescu, ChemElectroChem 2014, 1, 2082.
[8] O. Amor-Gutierrez, E. Costa Rama, A. Costa-Garcia, M. T. Fernandez-Abedul, Biosens. Bioelectron. 2017, 93, 40; O. Amor-Gutierrez, E. C. Rama, M. T. Fernandez-Abedul, A. Costa-Garcia, J. Chem. Educ. 2017, 94, 806; Y. Liu, V. Javvaji, S. R. Raghavan, W. E. Bentley, G. F. Payne, J. Agric. Food Chem. 2012, 60, 8963; X. Yang, D. Shi, S. Zhu, B. Wang, X. Zhang, G. Wang, ACS Sens. 2018, 3, 1368.
[9] M. K. Balaconis, K. Billingsley, M. J. Dubach, K. J. Cash, H. A. Clark, J Diabetes Sci Technol 2011, 5, 68; T. Elshaarani, H. Yu, L. Wang, A. Zain ul, R. S. Ullah, M. Haroon, R. Ullah Khan, S. Fahad, A. Khan, A. Nazir, M. Usman, K.-u.-R. Naveed, J. Mater. Chem. B 2018, 6, 3831; T. Lan, J. Zhang, Y. Lu, Biotechnol. Adv. 2016, 34, 331; H. Li, P. Dauphin-Ducharme, G. Ortega, K. W. Plaxco, J. Am. Chem. Soc. 2017, 139, 11207; A. Roy, S. Roy, A. Pradhan, S. Maiti Choudhury, R. Ranjan Nayak, Ind. Eng. Chem. Res. 2018, 57, 2847.
[10] X. H. Niu, L. B. Shi, H. L. Zhao, M. B. Lan, Anal. Methods 2016, 8, 1755.
[11] E. Bahcegul, E. Tatli, N. I. Haykir, S. Apaydin, U. Bakir, Bioresour. Technol. 2011, 102, 9646; J. P. Devadhasan, S. Kim, C. S. Choi, Analyst (Cambridge, U. K.) 2013, 138, 5679; J. Zhang, Y. Xiang, M. Wang, A. Basu, Y. Lu, Angew. Chem., Int. Ed. 2016, 55, 732.
[12] M.-S. Steiner, A. Duerkop, O. S. Wolfbeis, Chem. Soc. Rev. 2011, 40, 4805.
[13] L. C. Clark, Jr., C. Lyons, Ann. N. Y. Acad. Sci. 1962, 102, 29.
[14] S. J. Updike, G. P. Hicks, Nature (London) 1967, 214, 986; S. J. Updike, G. P. Hicks, Science (Washington, D. C.) 1967, 158, 270.
[15] K. E. Toghill, R. G. Compton, Int. J. Electrochem. Sci. 2010, 5, 1246.
[16] S. Park, H. Boo, T. D. Chung, Anal. Chim. Acta 2006, 556, 46.
[17] X. Niu, M. Lan, H. Zhao, C. Chen, Anal. Chem. (Washington, DC, U. S.) 2013, 85, 3561.
[18] J. Li, X. Lin, Biosens. Bioelectron. 2007, 22, 2898.
[19] R. Wilson, A. P. F. Turner, Biosens. Bioelectron. 1992, 7, 165.
[20] J. Kost, S. Mitragotri, R. A. Gabbay, M. Pishko, R. Langer, Nat. Med. (N. Y.) 2000, 6, 347; M. J. Tierney, J. A. Tamada, R. O. Potts, L. Jovanovic, S. Garg, Biosens. Bioelectron. 2001, 16, 621.
[21] J. C. Pickup, F. Hussain, N. D. Evans, O. J. Rolinski, D. J. S. Birch, Biosens. Bioelectron. 2005, 20, 2555; K. V. Larin, M. S. Eledrisi, M. Motamedi, R. O. Esenaliev, Diabetes Care 2002, 25, 2263; C. Zhang, G. G. Cano, P. V. Braun, Adv. Mater. (Weinheim, Ger.) 2014, 26, 5678.
[22] R. Weiss, Y. Yegorchikov, A. Shusterman, I. Raz, Diabetes Technol. Ther. 2007, 9, 68.
[23] L. D. Burke, Electrochim. Acta 1994, 39, 1841.
[24] F. Xie, Z. Huang, C. Chen, Q. Xie, Y. Huang, C. Qin, Y. Liu, Z. Su, S. Yao, Electrochem. Commun. 2012, 18, 108.
[25] A. Baciu, A. Pop, A. Remes, F. Manea, G. Burtica, Adv. Sci., Eng. Med. 2011, 3, 13.
[26] X. Zhong, R. Yuan, Y. Chai, Chem. Commun. (Cambridge, U. K.) 2012, 48, 597.

[27] J. Yuan, K. Wang, X. Xia, Adv. Funct. Mater. 2005, 15, 803; S. Park, T. D. Chung, H. C. Kim, Anal. Chem. 2003, 75, 3046; G. Wei, F. Xu, Z. Li, K. D. Jandt, J. Phys. Chem. C 2011, 115, 11453.
[28] Y.-Y. Song, D. Zhang, W. Gao, X.-H. Xia, Chem. - Eur. J. 2005, 11, 2177; K. Dawson, M. Baudequin, A. O'Riordan, Analyst (Cambridge, U. K.) 2011, 136, 4507.
[29] Y. Sun, H. Buck, T. E. Mallouk, Anal. Chem. 2001, 73, 1599.
[30] T. You, O. Niwa, Z. Chen, K. Hayashi, M. Tomita, S. Hirono, Anal. Chem. 2003, 75, 5191.
[31] M. Morita, O. Niwa, S. Tou, N. Watanabe, J. Chromatogr. A 1999, 837, 17; J. M. Marioli, T. Kuwana, Electroanalysis (N. Y.) 1993, 5, 11.
[32] P. F. Luo, T. Kuwana, Anal. Chem. 1994, 66, 2775.
[33] E. R. Kinser, J. Padmanabhan, R. Yu, S. L. Corona, J. Li, S. Vaddiraju, A. Legassey, A. Loye, J. Balestrini, D. A. Solly, J. Schroers, A. D. Taylor, F. Papadimitrakopoulos, R. I. Herzog, T. R. Kyriakides, ACS Sens. 2017, 2, 1779.
[34] C. Wang, L. Yin, L. Zhang, R. Gao, J. Phys. Chem. C 2010, 114, 4408; S. Hui, J. Zhang, X. Chen, H. Xu, D. Ma, Y. Liu, B. Tao, Sens. Actuators, B 2011, 155, 592.
[35] N. Karikalan, M. Velmurugan, S.-M. Chen, C. Karuppiah, ACS Appl. Mater. Interfaces 2016, 8, 22545; W. Mao, H. He, P. Sun, Z. Ye, J. Huang, ACS Appl. Mater. Interfaces 2018, 10, 15088; T. Chen, D. Liu, W. Lu, K. Wang, G. Du, A. M. Asiri, X. Sun, Anal. Chem. (Washington, DC, U. S.) 2016, 88, 7885; A. B. Urgunde, A. R. Kumar, K. P. Shejale, R. K. Sharma, R. Gupta, ACS Appl. Nano Mater. 2018, 1, 5571.
[36] H. Gleiter, Acta Mater. 2008, 56, 5875; J. X. Fang, U. Vainio, W. Puff, R. Wuerschum, X. L. Wang, D. Wang, M. Ghafari, F. Jiang, J. Sun, H. Hahn, H. Gleiter, Nano Lett. 2012, 12, 458; N. Chen, R. Frank, N. Asao, D. V. Louzguine-Luzgin, P. Sharma, J. Q. Wang, G. Q. Xie, Y. Ishikawa, N. Hatakeyama, Y. C. Lin, M. Esashi, Y. Yamamoto, A. Inoue, Acta Mater. 2011, 59, 6433; C. Benel, A. Fischer, A. Zimina, R. Steininger, R. Kruk, H. Hahn, A. Leon, Mater. Horiz. 2019, 6, 727; M. R. Chellali, S. H. Nandam, S. Li, M. H. Fawey, E. Moreno-Pineda, L. Velasco, T. Boll, L. Pastewka, R. Kruk, P. Gumbsch, H. Hahn, Acta Mater. 2018, 161, 47; O. Adjaoud, K. Albe, Acta Mater. 2016, 113, 284; O. Adjaoud, K. Albe, Acta Mater. 2018, 145, 322; N. Chen, D. V. Louzguine-Luzgin, K. Yao, J. Alloys Compd. 2017, 707, 371; C. Guo, Y. Fang, B. Wu, S. Lan, G. Peng, X.-l. Wang, H. Hahn, H. Gleiter, T. Feng, Mater. Res. Lett. 2017, 5, 293; D. V. Louzguine-Luzgin, S. V. Ketov, A. S. Trifonov, A. Y. Churymov, J. Alloys Compd. 2018, 742, 512; M. Sun, A. Rauf, Y. Zhang, G. Sha, G. Peng, Z. Yu, C. Guo, Y. Fang, S. Lan, T. Feng, H. Hahn, H. Gleiter, Mater. Res. Lett. 2018, 6, 55; C. Wang, D. Wang, X. Mu, S. Goel, T. Feng, Y. Ivanisenko, H. Hahn, H. Gleiter, Mater. Lett. 2016, 181, 248.
[37] M. Ghafari, H. Hahn, H. Gleiter, Y. Sakurai, M. Itou, S. Kamali, Appl. Phys. Lett. 2012, 101, 243104/1; R. Witte, T. Feng, J. X. Fang, A. Fischer, M. Ghafari, R. Kruk, R. A. Brand, D. Wang, H. Hahn, H. Gleiter, Appl. Phys. Lett. 2013, 103, 073106/1.
[38] N. Chen, X. Shi, R. Witte, K. S. Nakayama, K. Ohmura, H. Wu, A. Takeuchi, H. Hahn, M. Esashi, H. Gleiter, A. Inoue, D. V. Louzguine, J. Mater. Chem. B 2013, 1, 2568.
[39] S. H. Nandam, Y. Ivanisenko, R. Schwaiger, Z. Sniadecki, X. Mu, D. Wang, R. Chellali, T. Boll, A. Kilmametov, T. Bergfeldt, H. Gleiter, H. Hahn, Acta Mater. 2017, 136, 181.
[40] H. Gleiter, Beilstein J. Nanotechnol. 2013, 4, 517.
[41] W. H. Wang, C. Dong, C. H. Shek, Mater. Sci. Eng., R 2004, R44, 45.
[42] I. Singh, R. Narasimhan, Y. W. Zhang, Philos. Mag. Lett. 2014, 94, 678.

[43] N. Chen, D. Wang, T. Feng, R. Kruk, K.-F. Yao, D. V. Louzguine-Luzgin, H. Hahn, H. Gleiter, Nanoscale 2015, 7, 6607.
[44] D. Danilov, H. Hahn, H. Gleiter, W. Wenzel, ACS Nano 2016, 10, 3241.
[45] J. Q. Wang, N. Chen, P. Liu, Z. Wang, D. V. Louzguine-Luzgin, M. W. Chen, J. H. Perepezko, Acta Mater. 2014, 79, 30.
[46] J. Li, G. Doubek, L. McMillon-Brown, A. D. Taylor, Adv. Mater. (Weinheim, Ger.) 2019, 31.
[47] T. Kaneko, S. Tanaka, N. Asao, Y. Yamamoto, M. Chen, W. Zhang, A. Inoue, Adv. Synth. Catal. 2011, 353, 2927.
[48] G. Doubek, R. C. Sekol, J. Li, W.-H. Ryu, F. S. Gittleson, S. Nejati, E. Moy, C. Reid, M. Carmo, M. Linardi, P. Bordeenithikasem, E. Kinser, Y. Liu, X. Tong, C. O. Osuji, J. Schroers, S. Mukherjee, A. D. Taylor, Adv. Mater. (Weinheim, Ger.) 2016, 28, 1940.
[49] P. Zhang, Z. Wang, J. H. Perepezko, P. M. Voyles, J. Non-Cryst. Solids 2018, 491, 133; S. Jayalakshmi, V. S. Vasantha, E. Fleury, M. Gupta, Appl. Energy 2012, 90, 94; L. Yang, X.-f. Meng, G.-q. Guo, J. Mater. Res. 2013, 28, 3170.
[50] Z. Altounian, G. Tu, J. O. Strom-Olsen, J. Appl. Phys. 1983, 54, 3111; M. H. Enayati, E. Dastanpoor, Metall. Mater. Trans. A 2013, 44, 3984.
[51] M. H. Enayati, P. Schumacher, B. Cantor, J. Mater. Sci. 2002, 37, 5255.
[52] W. K. Luo, H. W. Sheng, F. M. Alamgir, J. M. Bai, J. H. He, E. Ma, Phys. Rev. Lett. 2004, 92, 145502/1; L. Sun, J. H. He, H. W. Sheng, P. C. Searson, C. L. Chien, E. Ma, J. Non-Cryst. Solids 2003, 317, 164.
[53] W. S. Lee, S. C. Kim, W. Y. Yoon, S. I. Kwun, Taehan Kumsok Hakhoechi 1996, 34, 886; G. Liang, E. Wang, Z. Li, Trans. Nonferrous Met. Soc. China 1994, 4, 83; G. Liang, E. Wang, X. Wang, Cailiao Kexue Yu Gongyi 1994, 2, 64; T. Nasu, K. Nagaoka, S. Takahashi, Yamagata Daigaku Kiyo, Kogaku 1990, 21, 43.
[54] J. Plummer, Nat. Mater. 2015, 14, 553.
[55] L. E. Collins, N. J. Grant, J. B. Vander Sande, J. Mater. Sci. 1983, 18, 804.
[56] A. S. Trifonov, A. V. Lubenchenko, V. I. Polkin, A. B. Pavolotsky, S. V. Ketov, D. V. Louzguine-Luzgin, J. Appl. Phys. (Melville, NY, U. S.) 2015, 117, 125704/1.

Graphical Abstract